Radiation Measurements 174 (2024) 107153

Contents lists available at ScienceDirect

Radiation Measurements

journal homepage: www.elsevier.com/locate/radmeas

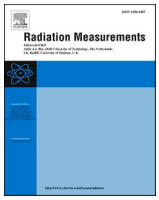

Radiophotoluminescence response of LiF:Mg,Ti pellets irradiated with clinical proton beams in the 70–200 MeV energy range

Massimo Piccinini [a,*], Alfredo Mirandola [b], Valentina Nigro [a], Maria Aurora Vincenti [a], Mario Ciocca [b], Rosa Maria Montereali [a]

[a] ENEA C.R. Frascati, Nuclear Department, Via E. Fermi 45, 00044, Frascati (Rome), Italy
[b] Centro Nazionale di Adroterapia Oncologica, Via Erminio Borloni 1, 27100, Pavia, Italy

ARTICLE INFO

Keywords:
Lithium fluoride
Color centers
TLD-100
Radiophotoluminescence
Proton beams
Protontherapy

ABSTRACT

Lithium fluoride doped with Mg and Ti (LiF:Mg,Ti) has been used for several decades as thermoluminescent dosimeter material, but recently also its radiophotoluminescence has been investigated for applications in dosimetry. In this work, LiF:Mg,Ti pellets (TLD-100) were irradiated in a water phantom at CNAO (Pavia, Italy) with therapeutic proton beams at five energies from 70 to 200 MeV in the dose range from 2 to 20 Gy. After irradiation, their visible radiophotoluminescence spectra were measured in controlled conditions and the spectrally-integrated red emission response of radiation-induced color centers has been investigated. The radiophotoluminescence signal, excited by a 445 nm continuous wave laser, was integrated within a 50 nm-wide band around the emission peak of the F_2 color centers, located around 670 nm in LiF. The spectrally-integrated signal of the samples irradiated at the energy of 147.7 MeV exhibited a linear dependence with dose. Moreover, this radiophotoluminescence response appears independent from Linear Energy Transfer in the range from 0.8 to 1.6 keV/μm in all the samples irradiated at the dose of 5 Gy. Such independence was found up to 10.3 keV/μm in samples irradiated within two spread out Bragg peaks made of 36 energy components in the entire investigated proton energy range. The radiophotoluminescence response of the TLD-100 pellets was compared to that of nominally-pure LiF crystals irradiated in the same conditions, which show a similar behavior. The results are encouraging for the exploitation of TLD-100 pellets as passive solid-state radiophotoluminescent dosimeters for proton therapy.

1. Introduction

Few wide-gap materials are suitable as passive solid-state radiation detectors based on radiophotoluminescence (RPL) of point defects and impurities contained in their crystalline matrix (Yanagida et al., 2022) with a wide range of applications in imaging and dosimetry (McKeever, 2022). Among them, crystalline oxides based on C and Mg doped sapphire (De Saint-Hubert et al., 2021) and silver activated phosphate glasses (Chang et al., 2017; Majer et al., 2024) are currently under investigation for dosimetry in hadrontherapy, to evaluate their RPL response with Linear Energy Transfer (LET) and dose, as it is known that solid state detectors change RPL efficiency as a function of LET in charged particle beams.

Doped lithium fluoride (LiF) has been successfully used for over 60 years as thermoluminescent dosimeter (Farrington et al., 1953; Horowitz, 2019), being highly sensitive at very low doses and water equivalent, but in the last two decades, it has been investigated for dosimetry applications of different radiation sources by exploiting RPL and optically stimulated luminescence (Oster et al., 2008, 2011, 2013; Marczewska et al., 2012; Piaskowska et al., 2013; Matsushima et al., 2013; Bilski et al., 2014). Irradiation of both doped and undoped LiF induces the formation of electronic defects, known as color centers (CCs), in the crystal lattice. Among them, the F_2 and F_3^+ CCs, consisting of two electrons bound to two and three close anion vacancies (Nahum and Wiegand, 1967), exhibit Stokes-shifted visible photoluminescence when excited with blue light (Baldacchini et al., 2000). Although the idea of using RPL for dosimetry is not new (Shulman et al., 1951), only recently the potential simplicity of a completely optical technique and the availability of sensitive enough, cheap and low-power consumption components for the RPL reading systems (Pollastrone et al., 2023) has made this research more intense. Our group has demonstrated the potential application in dosimetry of the RPL of stable F_2 CCs in

* Corresponding author.
E-mail address: massimo.piccinini@enea.it (M. Piccinini).

https://doi.org/10.1016/j.radmeas.2024.107153
Received 12 January 2024; Received in revised form 9 April 2024; Accepted 3 May 2024
Available online 3 May 2024

nominally-pure LiF crystals both at doses higher than 10^3 Gy with low-energy (3–7 MeV) proton beams (Piccinini et al., 2014) and, still more recently, at doses typical of radiotherapy with 35 MeV proton beams (Piccinini et al., 2020, 2023), as well as gamma rays from a reference ^{60}Co source (Piccinini et al., 2022) and 6 MV clinical X-rays (Villarreal-Barajas et al., 2015).

In this work, TLD-100 pellets and nominally-pure LiF crystals have been irradiated in a water phantom with clinical proton beams at several energies from 70 to 200 MeV in the dose range from 2 to 20 Gy. For both the pellets and the crystals, the visible RPL response of F_2 CCs, induced in the LiF crystalline matrix by the irradiation, has been investigated at room temperature as a function of dose and LET, with the aim of studying the possibility of using these materials as RPL-based passive dosimeters in proton therapy.

2. Materials and methods

Commercially-available (Harshaw, UK) TLD-100 pellets of diameter 4.5 mm and thickness 0.89 mm were irradiated with the scanning proton beams produced by the synchrotron installed at Centro Nazionale di Adroterapia Oncologica (CNAO) in Pavia (Italy), producing proton and carbon ion beams for treating patients since 2011 (Mirandola et al., 2015). The samples were placed inside a custom-made PMMA holder (see Fig. 1) that was mounted on the support bracket of the Markus chamber in a PTW 41023 water phantom (see Fig. 2); the samples position in the phantom was set in order to have an equivalent depth in water of 20 mm from the entrance beam position in the phantom (see inset of Fig. 2), corresponding to the plateau of the dose deposition Bragg curve. For each irradiation, three samples were irradiated simultaneously within a homogeneous field size of 6×6 cm^2 with a dose uniformity better than $\pm 1\%$ at a dose rate of 3 Gy/min.

A first set of irradiations was performed delivering a dose to water of 5 Gy at the proton beam energies of 70.21, 89.17, 119.47, 147.7, 196.7 MeV, covering the entire energy range commonly used for treatments. A second set of irradiations was performed at the intermediate beam energy of 147.7 MeV delivering doses of 2, 5, 10, 20 Gy. Finally, a third set of irradiations was performed placing the samples in the phantom within two different spread-out Bragg peaks (SOBPs). The first SOBP (SOBP#1, 6 cm thick, depth from 9 to 15 cm in water) was made of 36 isoenergetic slices in the range from 111 to 152 MeV and a total dose of 4 Gy was delivered. The second SOBP (SOBP#2, 6 cm thick, depth from 1 to 7 cm in water) was made of 36 isoenergetic slices in the range from 74 to 123 MeV with a 31 mm water-equivalent thick range shifter and a total dose of 6 Gy was delivered. The Treatment Planning System (TPS) RayStation v.11b (Raysearch Laboratories) was used to determine the dose-averaged LET (LET_D) values both at the depth of 20 mm, when the samples were irradiated at the five above-mentioned beam energies, and along the phantom depth, when the samples were irradiated in the two SOBPs.

Commercially-available (MacroOptica Ltd, Russia) 5×5 mm^2 and 0.5 mm-thick nominally-pure LiF crystals, with both square sides polished, were also irradiated in the same conditions and with the same irradiation parameters of the TLD-100 pellets.

After irradiation, all the samples were kept in darkness and a few days later, their RPL spectra were measured, consisting in the visible photoluminescence of the radiation-induced F_2 and F_3^+ CCs simultaneously excited in their overlapping absorption bands (Baldacchini et al., 2000) with a 10 mW and 1.53 mm beam-diameter continuous-wave (CW) laser at 445 nm, corresponding to the peak of the F_2 CCs absorption band (Baldacchini et al., 2000; Piccinini et al., 2020).

The RPL spectra were acquired by an Andor iDus 401 CCD cooled to −55 °C and attached to an Acton Research Spectra Pro 300i monochromator equipped with a 150 lines/mm grating and slits set at 1 mm; a Semrock BLP01-458R long-pass filter was placed in front of the entrance slits to prevent the laser light from entering the monochromator. The spectra acquisition time was 0.25 s for the TLD-100 pellets and 1 s for the LiF crystals. They were recorded 60 s after switching on the laser to allow stabilization of the F_3^+ CCs emission band, whose intensity initially decreases to a constant level due to the presence of a triplet state that traps a fraction of the excited electrons (Piccinini et al., 2022; Baldacchini et al., 1996). On the contrary, the F_2 CCs emission band is stable and in these conditions no RPL quenching is caused by the laser, thus allowing one repeating the measurements without any signal fading. Spectral analysis was carried on by OriginLab Origin 9.8 software.

3. Results and discussion

Fig. 3 shows the LET_D profile of the SOBPs as a function of depth in the water phantom, with highlighted positions of the LiF samples (square dots). In SOBP#1 the sample position (depth 11.4 cm) was chosen in an almost flat part of the LET_D profile with the corresponding value (2.5 keV/μm) just above the LET_D interval (from 0.8 to 1.6 keV/μm) of the five single beam energies. In SOBP#2 the sample position (depth 7 cm) was chosen in the distal part of the SOBP, where the LET_D profile is very steep and reaches a value one order of magnitude higher (10.3 keV/μm) than all the others. The LET_D values in the two SOBPs positions and at the depth of 2 cm for the five single beam energy values are reported in Table 1.

In Fig. 4, for each different combination of proton beam dose and energy values, the average of the RPL spectra of the three simultaneously irradiated samples are reported; they exhibit the typical superposition of the broad emission bands in the red and green spectral ranges, attributed to the F_2 and F_3^+ CCs, respectively. In the investigated measurement conditions, for all the spectra the intensity of the F_2 CCs band is much higher than that of the F_3^+ ones, as expected on the basis of the selected excitation wavelength (Baldacchini et al., 2000); moreover,

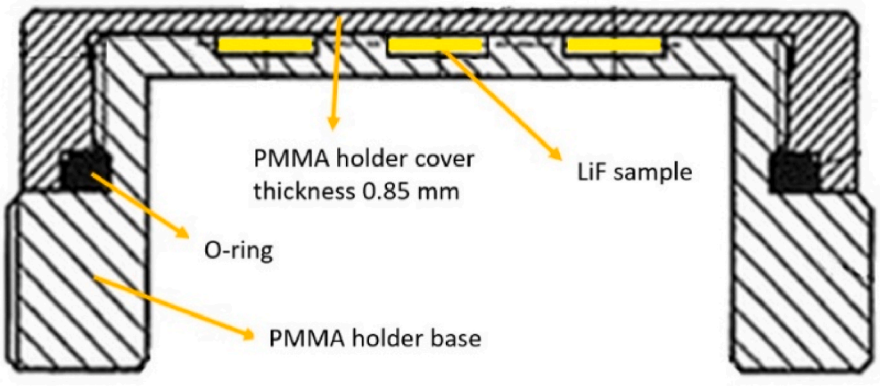

Fig. 1. Scheme of the PMMA LiF sample holder specifically designed for the water phantom.

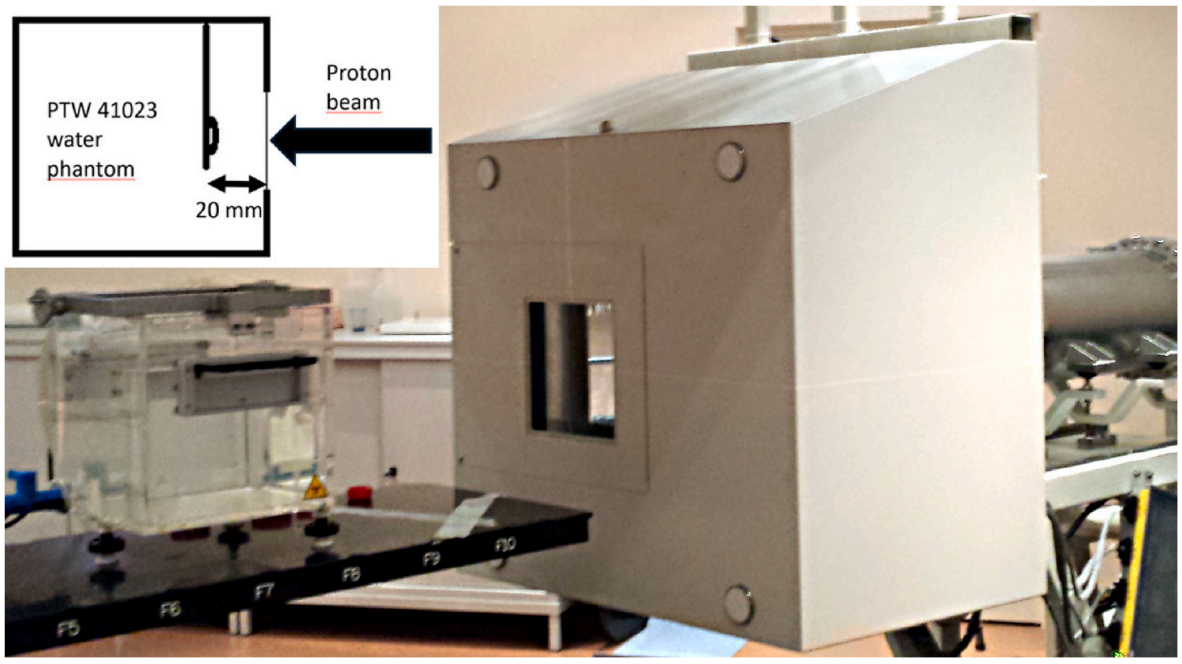

Fig. 2. Water phantom containing the LiF samples placed at the exit of the proton beamline and scheme (inset) showing the sample holder position inside the water phantom for all the irradiations, except those with SOBPs.

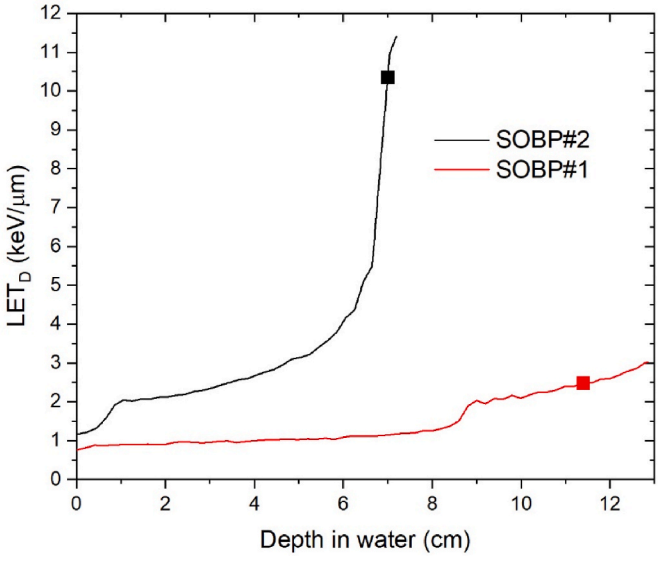

Fig. 3. Dose-averaged Linear Energy Transfer (LET_D) as a function of equivalent depth in water in the phantom of the SOBPs, with square dots marking the irradiated samples position.

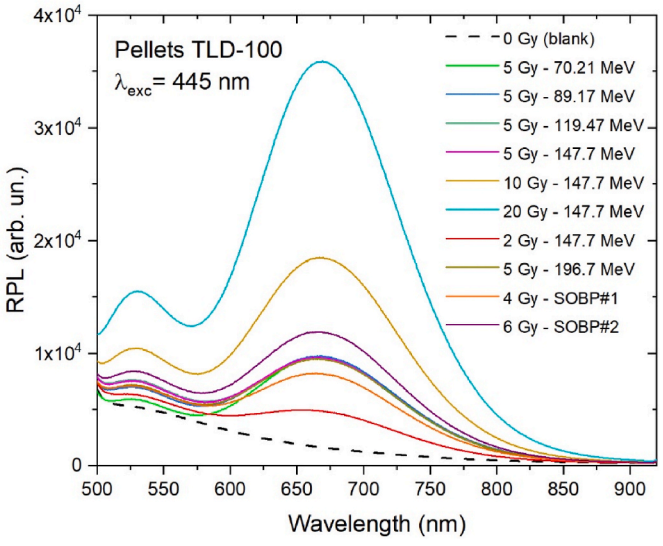

Fig. 4. Continuous wave laser excited (445 nm) RPL spectra (average of three simultaneously irradiated samples) of the TLD-100 pellets irradiated at several proton energies and doses.

Table 1
Dose averaged Linear Energy Transfer (LET_D) values and depths in the phantom for the samples irradiated with the single energy beams and in the SOBPs.

Energy (MeV)	LET_D (keV/μm)	Depth (cm)
70.21	1.6	2
89.17	1.2	2
119.47	1.0	2
147.7	0.9	2
196.7	0.8	2
111-152 (SOBP#1)	2.5	11.4
74-123 (SOBP#2)	10.3	7

around the peak of the F_2 CCs band (670 nm) the value of the average intrinsic luminescence of three not-irradiated samples (dashed line in Fig. 4) is very close to the minimum one, so around the peak of the red emission band the signal-to-noise ratio reaches its maximum value.

To exploit this maximum sensitivity and to avoid any contribution from the F_3^+ CCs band, the RPL signal has been integrated in a bandwidth of 50 nm around the emission peak at 670 nm. The spectrally-integrated RPL intensity of the samples irradiated with the beam of energy 147.7 MeV (LET_D = 0.9 keV/μm) as a function of the dose, in the entire considered dose range (2–20 Gy), is plotted in Fig. 5; such integrated RPL signal intensity is linear with dose, as shown by its linear best-fit. The error bars correspond to uncertainties of ±2σ (95% confidence).

The integrated RPL intensity of the TLD-100 samples irradiated at

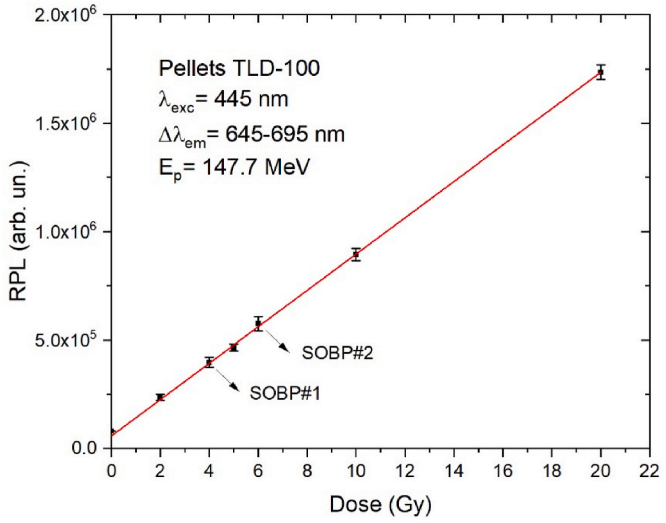

Fig. 5. Radiophotoluminescence intensity vs dose of TLD-100 pellets irradiated with 147.7 MeV protons and two SOBPs, obtained from the spectra shown in Fig. 4 integrated in the wavelength range 645–695 nm (average of three samples ±2σ) together with the linear best-fit (solid line).

the dose of 5 Gy at five values of the proton beam energy in the entire considered energy range (from 70.21 to 196.7 MeV, with a LET_D range from 0.8 to 1.6 keV/μm), is plotted in Fig. 6; it shows a RPL intensity independence from the LET_D within the measurement uncertainties with mean value for all the samples of 4.65×10^5 arb. units and $\sigma = 9.82 \times 10^3$ arb. units, corresponding to a relative error of 2.1%. Such independence from the LET_D is confirmed by the values obtained for the integrated RPL intensity of the samples irradiated within the two SOBPs at the dose values of 4 and 6 Gy (with LET_D of 2.5 and 10.3 keV/μm, respectively), which are also reported in the plot of Fig. 5. They were added after performing the linear best-fit of the RPL response of TLD-100 irradiated with almost mono-energetic proton beams. Within the measurement uncertainties, at these therapeutic dose values, their measured RPL response is the one that would be expected if they were irradiated with a beam of a single energy component within the entire range considered in this experiment; it means that the linear best-fit of Fig. 5 can be used as calibration for any proton beam energy in the investigated interval in the entire dose range from 2 to 20 Gy. This result can be considered a remarkable feature of the RPL response of TLD-100. As a matter of fact, both crystalline oxides based on C and Mg doped sapphire and silver activated phosphate glasses irradiated with therapeutic proton beams have shown RPL dependence with LET and need specific corrections for their non-linear RPL response with dose, especially for high LET values around the Bragg peak (De Saint-Hubert et al., 2021; Chang et al., 2017; Majer et al., 2024).

Nominally-pure LiF crystals were irradiated exactly in the same conditions of the TLD-100 pellets and also their RPL spectra were measured with the same spectrometric system under identical laser pumping excitation. As expected, their RPL spectra (data not shown) exhibited similar spectral characteristics of those of the TLD-100 pellets and the spectrally-integrated F_2 CCs RPL intensity was derived (see Figs. 7 and 8). Also for the proton-irradiated LiF crystals the RPL response is linear with dose; it is independent from the LET_D within the measurement uncertainties with mean value for all the samples of 1.88×10^5 arb. units and $\sigma = 1.41 \times 10^4$ arb. units, corresponding to a relative error of 7.5%, which is about four times higher than that of the pellets. In fact, the error bars of the RPL signal in the crystals are often bigger than those in the pellets (see Figs. 7 and 5, respectively). It should be considered that scattering effects of the pumping laser light through the pressed powder of the pellets, characterized by a microcrystalline structure and a thickness about twice that of the crystals, allows the excitation of a larger sample volume thus giving rise to a RPL signal about ten times higher in pellets, resulting in a more stable signal acquired by the CCD with the same acquisition time.

Comparing the data of Figs. 5–8 we can derive that the RPL linear response of LiF is not significantly affected by the presence of dopants at the concentrations typical of the TLD-100 pellets, although it may influence their sensitivity. It should be noticed that the linear dependence of the RPL with dose, observed both in the TLD-100 pellets and in the nominally-pure LiF crystals irradiated with clinical protons from 70 to 200 MeV, had been already observed in LiF crystals irradiated with a 6 MV X-ray clinical beam up to 100 Gy (Villarreal-Barajas et al., 2015), with 35 MeV protons up to 50 Gy (Piccinini et al., 2020), with 3 MeV protons up to 2×10^5 Gy (Piccinini et al., 2023) and with a reference ^{60}Co gamma beam in the dose range from 1 to 20 Gy (Piccinini et al., 2022). Moreover, the full Bragg curve of a 26 MeV proton beam could be directly imaged by fluorescence microscopy of CCs in nominally-pure LiF crystals. Best-fitting the curve with an analytical model of LET in

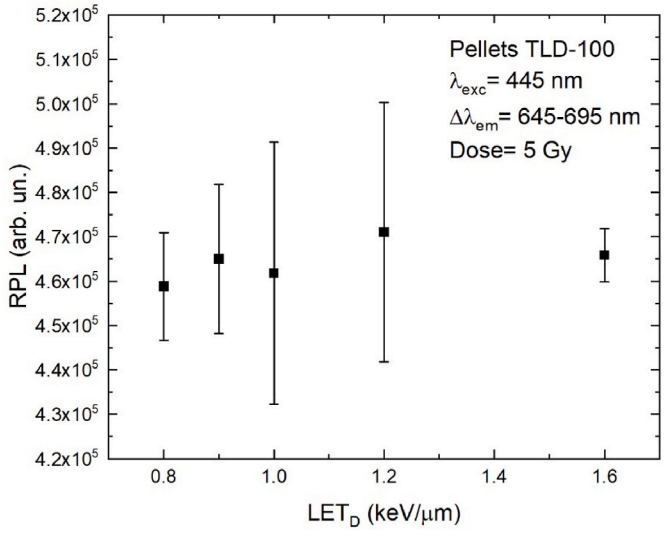

Fig. 6. Radiophotoluminescence intensity vs LET_D of TLD-100 pellets irradiated at a dose of 5 Gy, obtained from the spectra shown in Fig. 4 integrated in the wavelength range 645–695 nm (average of three samples ±2σ).

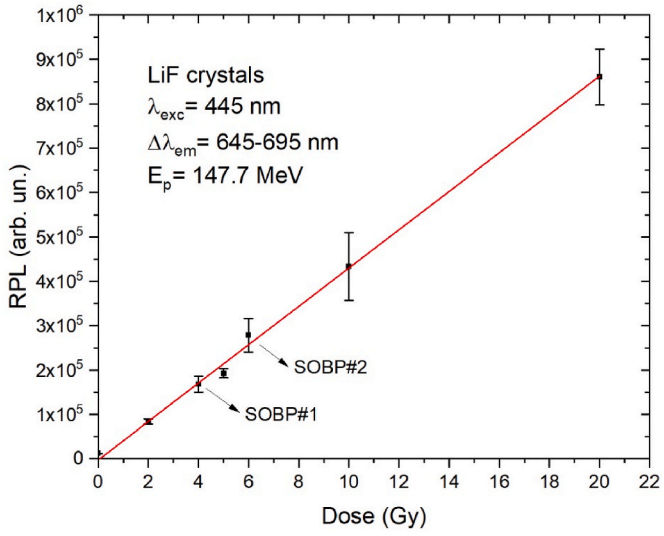

Fig. 7. Radiophotoluminescence intensity vs dose of nominally-pure LiF crystals irradiated with 147.7 MeV protons and two SOBPs, obtained from the spectra (not shown) integrated in the wavelength range 645–695 nm (average of three samples ±2σ) together with the linear best-fit (solid line).

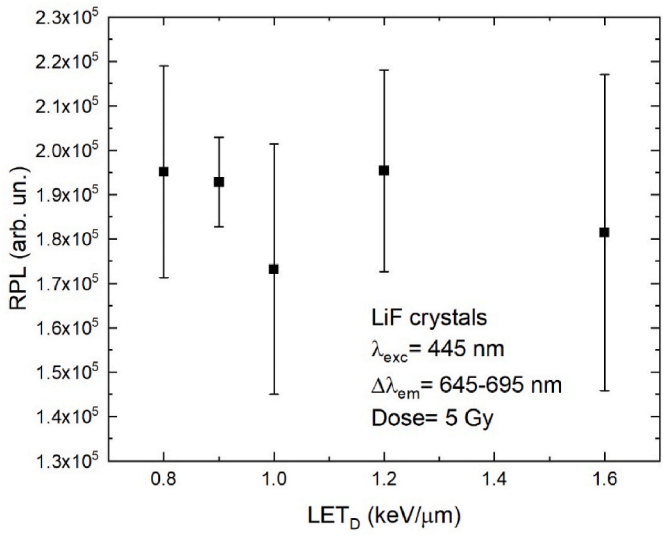

Fig. 8. Radiophotoluminescence intensity vs LET_D of nominally-pure LiF crystals irradiated at a dose of 5 Gy, obtained from the spectra (not shown) integrated in the wavelength range 645–695 nm (average of three samples ±2σ).

LiF allowed estimating the beam energy parameters and demonstrated the RPL independence from the LET along the entire Bragg curve (Piccinini et al., 2020).

4. Conclusions

Passive solid state dosimeters, consisting of TLD-100 pellets, are well-known for applications in thermoluminescence dosimetry, characterized by very high sensitivity ($<10^{-4}$ Gy) and tissue equivalence, which is essential for meaningful medical applications. Only very recently, their RPL response was investigated for dosimetry applications with therapeutic doses. In this study, TLD-100 pellets were irradiated in controlled conditions with clinical proton beams at fixed energies in the 70–200 MeV energy range and in a dose interval from 2 to 20 Gy at the CNAO synchrotron for proton therapy. Their laser-excited visible RPL spectra, integrated in a 50 nm-wide interval centered on the F_2 CCs red emission peak, exhibited a linear behavior as a function of the absorbed dose (to water). Moreover, the integrated RPL signal is independent from LET in the range from 0.8 to 10.3 keV/μm, as resulted from samples irradiated with both mono-energetic beams and within two SOBPs made of 36 isoenergetic slices in the entire investigated proton energy range at typical clinical doses. Similar behaviors were found for the RPL response of LiF crystals irradiated in the same clinical conditions. Both these characteristics are very promising for their use as passive solid-state photoluminescent dosimeters for proton therapy. Further investigations on the time stability of CCs in both TLD-100 and LiF crystals are necessary, but their RPL sensitivity at typical therapeutic doses and the obtained results are very encouraging, also in the perspective to combine RPL measurements with the absorbed dose evaluation performed by exploiting thermoluminescence in the TLD-100 pellets and for their re-usability.

CRediT authorship contribution statement

Massimo Piccinini: Writing – review & editing, Writing – original draft, Validation, Methodology, Investigation, Formal analysis, Data curation, Conceptualization. **Alfredo Mirandola:** Writing – review & editing, Validation, Methodology, Data curation. **Valentina Nigro:** Writing – review & editing, Methodology, Conceptualization. **Maria Aurora Vincenti:** Writing – review & editing, Methodology, Conceptualization. **Mario Ciocca:** Writing – review & editing, Supervision, Resources, Methodology, Conceptualization. **Rosa Maria Montereali:** Writing – review & editing, Writing – original draft, Supervision, Resources, Methodology, Investigation, Conceptualization.

Declaration of competing interest

The authors declare that they have no known competing financial interests or personal relationships that could have appeared to influence the work reported in this paper.

Data availability

Data will be made available on request.

Acknowledgements

Research carried out within the TECHEA (TEChnologies for HEAlth) project, funded by ENEA, Italy. The authors would like to thank Prof. Jose Eduardo Villarreal-Barajas (Royal Devon and Exeter NHS Foundation Trust) for his valuable suggestions and fruitful discussions.

References

Baldacchini, G., Cremona, M., d'Auria, G., Montereali, R.M., Kalinov, V., 1996. Radiative and nonradiative processes in the optical cycle of the F_3^+ center in LiF. Phys. Rev. B 54, 17508.
Baldacchini, G., De Nicola, E., Montereali, R.M., Scacco, A., Kalinov, V., 2000. Optical bands of F_2 and F_3^+ centers in LiF. J. Phys. Chem. Solid. 61, 21.
Bilski, P., Marczewska, B., Twardak, A., Mandowska, E., Mandowski, A., 2014. OSL signal of lithium fluoride and its relationship with TL glow-curves. Radiat. Meas. 71, 61–64.
Chang, W., Koba, Y., Katayose, T., Yasui, K., Omachi, C., Hariu, M., Saitoh, H., 2017. Correction of stopping power and LET quenching for radiophotoluminescent glass dosimetry in a therapeutic proton beam. Phys. Med. Biol. 62 (23), 8869.
De Saint-Hubert, M., Castellano, F., Leblans, P., Sterckx, P., Kodaira, S., Swakoń, J., de Freitas Nascimento, L., 2021. Characterization of 2D Al2O3: C, Mg radiophotoluminescence films in charged particle beams. Radiat. Meas. 141, 106518.
Farrington, D., Boyd, C.A., Saunders, D.F., 1953. Thermoluminescence as a research tool. Science 117, 343–349.
Horowitz, Y.S., 2019. Thermoluminescence and Thermoluminescence Dosimetry, vol. 3. CRC Press. ISBN-13978-0367262617.
Majer, M., Pasariček, L., Brkić, H., Davídková, M., Navrátil, M., Vondráček, V., Knezević, Z., 2024. Relative efficiency of radiophotoluminescent glass dosimeters in a scanning pencil proton beam. Radiat. Phys. Chem. 216, 111396.
Marczewska, B., Bilski, P., Mandowska, E., Mandowski, A., 2012. Photoluminescence of gamma, proton and alpha-irradiated LiF detectors. Cent. Eur. J. Phys. 10 (4), 1009–1012.
Matsushima, L.C., Veneziani, R.G., Campos, L.L., 2013. Study of optically stimulated luminescence of LiF:Mg,Ti for beta and gamma dosimetry. Radiat. Meas. 56, 365–368.
McKeever, S., 2022. A Course in Luminescence Measurements and Analyses for Radiation Dosimetry. John Wiley & Sons Ltd.. ISBN: 978-1-119-64689-1.
Mirandola, A., Molinelli, S., Vilches Freixas, G., Mairani, A., Gallio, E., Panizza, D., Russo, S., Ciocca, M., Donetti, M., Magro, G., Giordanengo, S., Orecchia, R., 2015. Dosimetric commissioning and quality assurance of scanned ion beams at the Italian National Center for Oncological Hadrontherapy. Med. Phys. 42 (9), 5287–5300.
Nahum, J., Wiegand, D.A., 1967. Optical properties of some F-aggregate centers in LiF. Phys. Rev. 154 (3), 817.
Oster, L., Horowitz, Y.S., Podpalov, L., 2008. OSL and TL in LiF:Mg,Ti following alpha particle beta ray irradiation: application to mix field radiation dosimetry. Radiat. Protect. Dosim. 128 (3), 261–265.
Oster, L., Druzhyna, S., Horowitz, Y.S., 2011. Optically stimulated luminescence in LiF: Mg,Ti: application to solid state radiation dosimetry. Nucl. Instrum. Methods 648, 261–265.
Oster, L., Druzhyna, S., Orion, I., Horowitz, Y.S., 2013. Study of combinations of TL/OSL single dosimeters for mixed high/low ionization density radiation fields. Radiat. Meas. 56, 320–323.
Piaskowska, A., Marczewska, B., Bilski, P., Mandowski, A., Mandowska, E., 2013. Photoluminescence measurements of LiF TL detectors. Radiat. Meas. 56, 209–212.
Piccinini, M., Ambrosini, F., Ampollini, A., Carpanese, M., Picardi, L., Ronsivalle, C., Bonfigli, F., Libera, S., Vincenti, M.A., Montereali, R.M., 2014. Solid state detectors based on point defects in lithium fluoride for advanced proton beam diagnostics. J. Lumin. 156, 170.
Piccinini, M., Nichelatti, E., Ampollini, A., Bazzano, G., De Angelis, C., Della Monaca, S., Nenzi, P., Picardi, L., Ronsivalle, C., Surrenti, V., Trinca, E., Vadrucci, M., Vincenti, M.A., Montereali, R.M., 2020. Dose response and Bragg curve reconstruction by radiophotoluminescence of color centers in lithium fluoride

crystals irradiated with 35 MeV proton beams from 0.5 to 50 Gy. Radiat. Meas. 133, 106275.
Piccinini, M., Nichelatti, E., Pimpinella, M., De Coste, V., Montereali, R.M., 2022. Dose response of visible color center radiophotoluminescence in lithium fluoride crystals irradiated with a reference ^{60}Co gamma beam in the 1–20 Gy dose range. Radiat. Meas. 151, 106705.
Piccinini, M., Nichelatti, E., Vincenti, M.A., Nigro, V., Ronsivalle, C., Ampollini, A., Nenzi, P., Bazzano, G., Trinca, E., Montereali, R.M., 2023. Dynamic range and dose linearity of the radiophotoluminescence intensity in lithium fluoride crystals irradiated with 2.3 and 26 MeV protons. Radiat. Meas. 259, 119833.
Pollastrone, F., Piccinini, M., Pizzoferrato, R., Palucci, A., Montereali, R.M., 2023. Fully-digital low-frequency lock-in amplifier for photoluminescence measurements. Analog Integr. Circuits Signal Process 115, 67.
Shulman, J.H., Ginther, R.J., Click, C.C., Alger, R.S., Levy, R.A., 1951. Dosimetry of X-rays and gamma by radiophotoluminescence. J. Appl. Phys. 22 (12), 1479.
Villarreal-Barajas, J.E., Piccinini, M., Vincenti, M.A., Bonfigli, F., Khan, R.F., Montereali, R.M., 2015. Visible photoluminescence of color centers in LiF crystals for absorbed dose evaluation in clinical dosimetry. IOP Conf. Ser. Mater. Sci. Eng. 80, 12020.
Yanagida, T., Okada, G., Kato, T., Nakauchi, D., Kawaguchi, N., 2022. A review and future of RPL dosimetry. Radiat. Meas. 158, 106847.